Monthly Notices
of the
ROYAL ASTRONOMICAL SOCIETY

MNRAS **475,** 3086–3089 (2018)
Advance Access publication 2018 January 10

doi:10.1093/mnras/sty078

A closer look at the quadruply lensed quasar PSOJ0147: spectroscopic redshifts and microlensing effect

Chien-Hsiu Lee (李見修)★

Subaru Telescope, National Astronomical Observatory of Japan, 650 North A'ohoku Place, Hilo, HI 96720, USA

Accepted 2018 January 5. Received 2017 December 19; in original form 2017 November 2

ABSTRACT

I present a timely spectroscopic follow-up of the newly discovered, quadruply lensed quasar PSOJ0147 from the Pan-STARRS 1 survey. The newly acquired optical spectra with GMOS onboard the Gemini North Telescope allow us to pin down the redshifts of both the foreground lensing galaxy and the background lensed quasar to be $z = 0.572$ and 2.341, providing a firm basis for cosmography with future high-cadence photometric monitoring. I also inspect difference spectra from two of the quasar images, revealing the microlensing effect. Long-term spectroscopic follow-ups will shed lights on the structure of the active galactic nucleus and its environment.

Key words: gravitational lensing: strong – quasars: general – cosmology: observation.

1 INTRODUCTION

In the context of precision cosmology, determining the local value of H_0 to a percent level and comparing it with cosmic microwave background (CMB) results provides a tremendous leverage on the dark energy, neutrino physics, and the geometry of the Universe. Taking advantage of the distance ladder, the SH0ES team obtained a local measurement of H_0 to 2.4 per cent (Riess et al. 2016) is in tension (at the 3.4σ level) with the *Planck* CMB results. Before claiming that such tension is due to systematics in the *Planck* measurement, or hints to new physics, it is important to have independent local H_0 measurements with a comparable precision.

In this regard, the gravitational lensing time-delay method is an ideal alternative. This is because in strong lensing, lights from a multiple-image source will go through different paths (geodesics). Since light traveltimes (or time-delays) differ proportionally to the space–time curvature, we can thus estimate the H_0. Refsdal (1964) originally suggested to use standard candles such as supernovae to measure the time-delay. Supernovae, especially of Type Ia (SNe Ia), have several advantages in time-delay measurements (see e.g. Lee 2017). First of all, SNe Ia have a distinct light-curve shape, so we can measure the time-delay accurately if they are discovered and followed up well before the light maximum. Secondly, from the empirical light curve template, we know the intrinsic brightness of the SNe, which provides the *magnification factor* that breaks the mass–sheet degeneracy and yields a direct measurement of H_0 (Oguri & Kawano 2003). However, due to the lack of all-sky transient surveys, the first multiply lensed SN Ia, iPTF16geu, was reported only very recently (Goobar et al. 2017). The discovery of iPTF16geu demonstrated that it is very difficult to establish the lensing nature before the SN light maximum, making it difficult to measure time-delays. To make it worse, lensed SNe Ia will also suffer from microlensing effects (More et al. 2017), further accurate determination of the time delay. In this regard, instead of SNe Ia, time-delay measurements were carried out with quasars as a background source. For example, the most recent time-delay measurements from the H0LiCOW team (Suyu et al. 2017) demonstrated that it is possible to measure time-delays with three multiply lensed quasars, enabling an H_0 estimation at 3.8 per cent level (Bonvin et al. 2017). This was possible because they also constrained the mass–sheet effect with spectroscopic observations (Rusu et al. 2017), thus were able to break the constraint of the effect of external masses along the line of sight.

Although the current time-delay method provides a consistent H_0 estimate like the distance ladder method, we still need to obtain H_0 to the 1 per cent level, both to understand the tension with the CMB results from the *Planck* satellite and to shed light on the dark energy. However, at present there are only a handful of suitable multiply lensed systems; hence, we need to increase the sample of suitable lensed quasars. Recently, Berghea et al. (2017) have identified a new quadruply lensed quasar candidate from the Pan-STARRS archive data. This system is of particular interests because the four lensed quasar images are bright and provide a potentially suitable case for accurate time-delay measurements. This is especially the case when we consider to adopt the new high-cadence monitoring method proposed by Courbin et al. (2017).

In this work, I present timely follow-up spectra of this new candidate, with the aim to provide accurate redshifts of both the foreground lensing galaxy and the background quasar for cosmography. This paper is organized as follows: The observation is documented in Section 2. The analysis and results are presented in Section 3. I give the conclusion in Section 4.

★ E-mail: leech@naoj.org

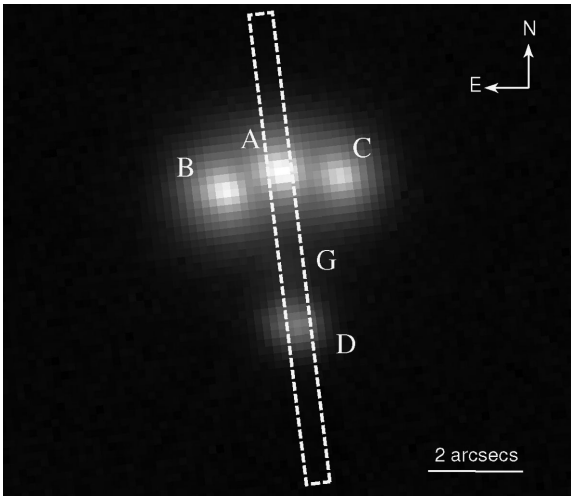

Figure 1. Illustration of the GMOS-N spectroscopic follow-up. The lensed quasar images are marked in A–D, starting with the brightest image A ($i = 15.40$ mag). The 0.5-arcsecslit is shown in a violet rectangle. With a single slit position (position angle $= 7^{\circ}$), we can obtain spectra of the brightest and faintest quasar image as well as of the lensing galaxy at once. The background image is a 10-s acquisition exposure in the i band from GMOS-N, showing a region of 10×10 arcsec^2, where north is up and east is to the left.

2 OBSERVATION

PSOJ0147 was first reported by Berghea et al. (2017), but was invisible for an immediate follow-up at that time, and Berghea et al. (2017) derived only the redshifts of the foreground lens and the background quasar photometrically.

Although the lensed images are rather bright, with $i = 15.40$–17.74 mag, the foreground lens is rather faint, with $i = 19.5$ mag. Though Rubin et al. (2017) carried out spectroscopic observations of the lensed quasars with the Keck Cosmic Web Imager (KWCI) onboard the Keck II telescope, they only obtained a total integration time of ∼1200 s, not deep enough to detect the foreground lensing galaxy. Furthermore, Rubin et al. (2017) covered only the blue side of the optical spectrum; hence, their redshift estimate of $z = 2.377$ is heavily influenced by the broad absorption line (BAL) feature. Indeed, a broader wavelength coverage from the 2.5-m Nordic Optical Telescope (Lee 2017) provides a more accurate redshift estimate using the cleaner forbidden line [C III], resulting in a smaller quasar redshift of $z = 2.341 \pm 0.001$. However, neither Rubin et al. (2017) nor Lee (2017) was able to detect the foreground lens spectroscopically. In this regard, I thus made use of the fast turnaround programme of the 8-m Gemini North Telescope at Maunakea, with its Gemini Multi Object Spectrograph (GMOS-N). To reveal the spectral feature of the faint foreground lensing galaxy, I obtained 4×1200-s exposures with a 0.5-arcsec slit to cover the foreground lensing galaxy, as well as the brightest and faintest quasar images (see Fig. 1). The observations were carried out with the B600 grating to cover a wide wavelength range in the optical. Given the photometric redshift of the foreground lens at $z = 0.57$, I expected to cover the Ca H&K lines, as well as the G-band absorption features. In addition, with the background quasar at $z = 2.341$, I expected to cover the [C III] λλ 1908.734 Å forbidden line, to verify the redshift of the quasar, as reported by Lee (2017).

The observations were carried out on 2017 September 2 with GMOS-N mounted on the Gemini North Telescope (programme ID: GN-2017B-FT-4). To avoid bad pixels and remove cosmic rays, the observations were performed using an A–B–B–A sequence, with a 1 arcsec dithering. We took 1200-s exposures at each dithering position, resulting in a total integration time of 80 min.

Data reductions were carried out in a standard fashion using IRAF[1] and the Gemini IRAF package,[2] including subtraction of bias, flat-fielding, calibrating the wavelength using a Thorium–Argon lamp, and calibrating the flux using a spectroscopic standard star EG 131.

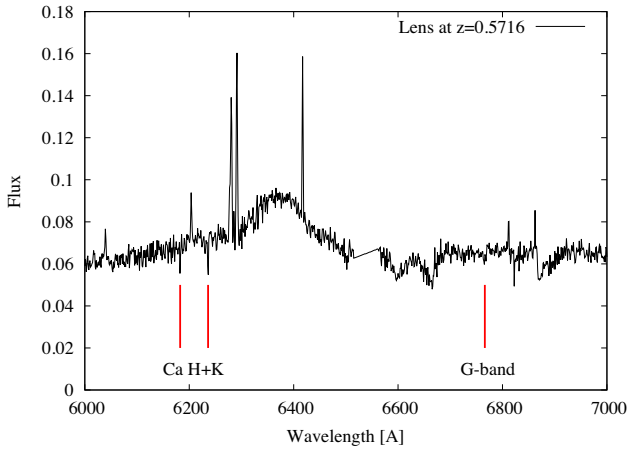

Figure 2. Spectrum of the foreground lensing galaxy from GMOS-N onboard the Gemini North Telescope. Absorption features, such as the Ca H λλ3934, Ca K λλ3969, and G-band λλ4304, are marked with red labels, assuming a redshift of 0.5716. Note that the lens galaxy and the lensed images of the background quasar are very close; thus, the lens galaxy spectrum is blended by the light from the quasar images. Nevertheless, this does not affect the redshift determination of the lens galaxy, as we can clearly see the absorption lines from the lens galaxy

Table 1. Gaussian centroid of absorption features in the lens spectrum.

Lines	λ_{obs} (Å)	z
Ca H λλ3934	6182.68	0.5716
Ca K λλ3969	6236.02	0.5712
G- band λλ4304	6766.1	0.5720

3 RESULTS

After data reduction, I can see traces of absorption lines from the foreground lensing galaxy, e.g. Ca H&K (λλ3934, 3969) and G band (λλ4304). The reduced lens spectrum, as well as these absorption features, is shown in Fig. 2. From these absorption features, I am able to obtain the lens redshift; I use the *splot* task in IRAF, and perform a Gaussian fitting to the Ca H&K and G-band features. After measuring the Gaussian centroids from each image, I use their mean to determine the redshift, and the standard deviation as the redshift uncertainty, resulting in a redshift $z = 0.5716 \pm 0.0004$. The values of the Gaussian centroid from each of the absorption features are shown in Table 1.

In addition to the lens, I also obtained spectra of the brightest and the faintest quasar images (A and D). After reduction, I clearly see

[1] IRAFis distributed by the National Optical Astronomy Observatory, which is operated by the Association of Universities for Research in Astronomy (AURA) under a cooperative agreement with the National Science Foundation.
[2] http://www.gemini.edu/node/11823

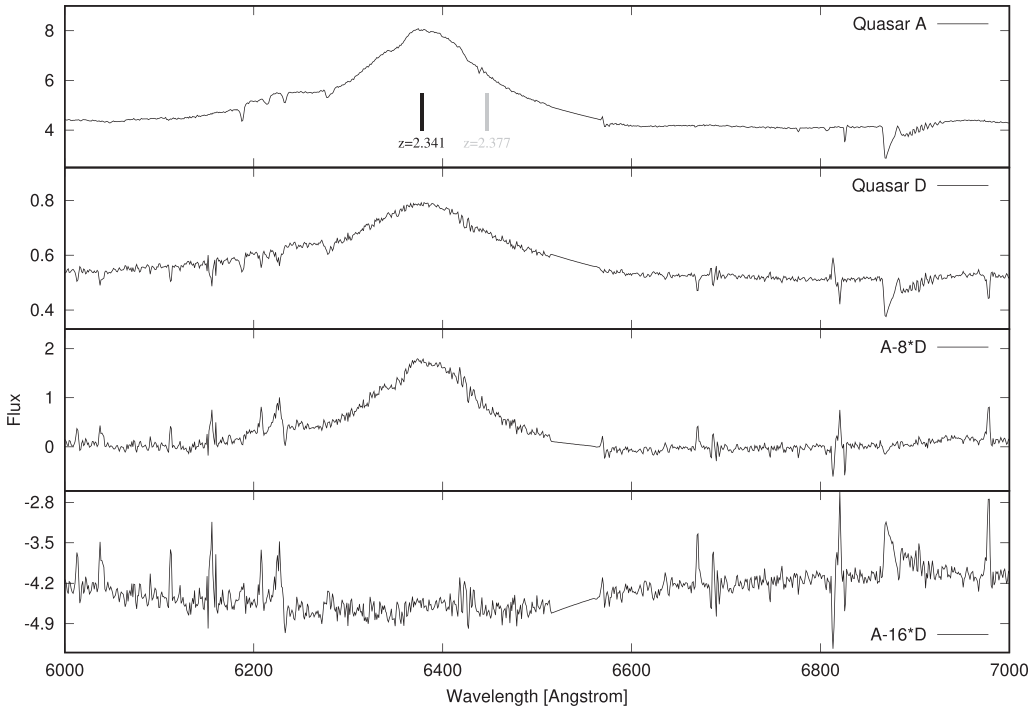

Figure 3. From the top to bottom: (1) spectrum of the brightest quasar image A, showing the [C III] emission line around 6380 Å (marked by the black label), confirming the quasar to be at $z = 2.341$. If the quasar were at $z = 2.377$ as Rubin et al. suggested, the [C III] emission line would be at 6447 Å (marked by the grey label), completely offset from the peak of the [C III] emission line shown in the plot; (2) spectrum of the faintest quasar image D, with the [C III] emission line around 6380 Å; (3) difference spectrum of image A – 8× the flux of image D, nulling the flux contribution from the continuum and revealing only the flux contribution from the [C III] emission line; and (4) difference spectrum of image A – 16× the flux of image D, nulling the flux contribution from the [C III] emission line and revealing only the flux contribution from continuum. I can see a residual continuum bluewards of the [C III] emission line, suggesting microlensing effect.

the [C III] forbidden emission line, as shown in Fig. 3. As [C III] is free from BALs, it is ideal to be used to estimate redshifts. Indeed, Lee (2017) reported a quasar redshift of 2.341±0.001, contrasting to earlier results from Rubin et al. (2017). As discussed in Lee (2017), the differences may originate from the shorter wavelength coverage, as well as contaminations from BALs in Rubin et al. (2017). Here, with the new Gemini/GMOS-N spectra, I again confirm [C III] of the background quasar peaks at ∼6380 Å, suggesting that the background quasar is at $z = 2.341$, in agreement with the results from Lee (2017) and smaller than the results from Rubin et al. (2017).

With the spectra from quasar images A and D at hand, I can also investigate the microlensing effect spectroscopically using difference spectrum. This has been done; for example, Wisotzki, Koehler & Kayser (1993) and Lidman et al. (2000) have investigated the difference spectra of the doubly lensed system HE 1104 − 1805, and revealed the microlensing effects from spectra. Furthermore, Sluse et al. (2012) presented a spectroscopic microlensing for 17 lensed quasars. If microlensing affects the spectra, there will exist a factor K where spectrum A − K times spectrum D will cancel out the continuum and I can see only the emission line. In addition, there will also exist another K value where the emission lines will be cancelled out and leave only a blue residual continuum since microlensing affects most the central parts of the accretion disc. By experimenting different values of K, with $K = 8$, I am able to null the continuum and leave only the emission features. With $K = 16$, I can cancel out the emission feature, leaving a blue residual continuum. The difference spectra are shown in Fig. 2. These suggest that we can see traces of the microlensing effects in PSOJ0147. The continuum is more susceptible to microlensing effects. Taking the flux ratio between the continuum of images A and D, I obtain a magnitude difference of 2.26 mag, close to the value of the observed quasar image magnitudes relative to image A, in particular the r band around 2.3 mag for image D versus image A, as shown in fig. 7 of Berghea et al. (2017). On the other hand, the emission-line flux ratio of images A and D suggests a magnitude difference of 3.01 mag, in the same direction (larger magnitude difference) as predicted by the lens modelling of Berghea et al. (2017).

4 CONCLUSIONS

PSOJ0147 is the first quadruply lensed quasar candidate identified in the Pan-STARRS archive data. In this paper, I present follow-up spectra of PSOJ0147 using GMOS-N onboard the Gemini North Telescope. The results can be summarized as follows:

(i) *I provided the first spectrum of the foreground lensing galaxy.* As the foreground lensing galaxy is very faint ($i = 19.5$ mag), a previous spectroscopic follow-up by Rubin et al. (2017) could not reveal the spectral signature of the foreground lens. With the power of the 8-m Gemini telescopes, and with a total integration time of 80 min, I was able to obtain a spectrum of the foreground lensing galaxy for the first time. Using Ca H&K and G band, I was able to determine the lens redshift to be $z = 0.5716$, close to the photo-z prediction by Berghea et al. (2017).

(ii) *I confirmed the background quasar at a redshift of* $z = 2.341$. For cosmographical studies, it is crucial to obtain accurate spectroscopic redshifts of both the foreground lens and the background quasar. Contrasting with the results of Lee (2017), a previous study

by Rubin et al. (2017) reported a larger redshift of the background quasar at $z = 2.377$, which is likely to be affected by the BAL nature of the background quasar, and the narrow wavelength coverage (up to C IV at the observer's frame) in Rubin et al. (2017). Here, with the prominent [C III] emission-line peaks at 6380 Å, I confirmed the background quasar at $z = 2.341$.

(iii) *I demonstrated the microlensing effect in difference spectra.* As microlensing affects most of the central parts of the accretion disc, the continuum and the emission component of the background quasar will experience different lensing factors. I investigated the difference spectra between quasar images A and D, and showed that with A − 8×D we can null the continuum, whereas with A − 16×D we can cancel out the emission-line feature. Further epochs of a spectroscopic monitoring will be crucial to study the environment around the active galactic nucleus of the background quasar.

ACKNOWLEDGEMENTS

C-HL is indebted to the referee, whose comments greatly improved the manuscript.

Based on observations (GN-2017B-FT-4) obtained at the Gemini Observatory and processed using the Gemini IRAF package, which is operated by the Association of Universities for Research in Astronomy, Inc., under a cooperative agreement with the NSF on behalf of the Gemini partnership: the National Science Foundation (United States), the National Research Council (Canada), CONICYT (Chile), Ministerio de Ciencia, Tecnología e Innovación Productiva (Argentina), and Ministério da Ciência, Tecnologia e Inovação (Brazil).

The author wishes to recognize and acknowledge the very significant cultural role and reverence that the summit of Maunakea has always had within the indigenous Hawaiian community and is very fortunate to have the opportunity to conduct observations from this mountain.

REFERENCES

Berghea C. T., Nelson G. J., Rusu C. E., Keeton C. R., Dudik R. P., 2017, ApJ, 844, 90
Bonvin V. et al., 2017, MNRAS, 465, 4914
Chambers K. C. et al., 2016, preprint (arXiv:1612.05560)
Courbin F. et al., 2017, preprint (arXiv:1706.09424)
Goobar A. et al., 2017, Science, 356, 291
Lee C.-H., 2017, A&A, 605, L8
Lee C.-H., 2017, Nature Astron., 1, 0155
Lidman C., Courbin F., Kneib J.-P. et al., 2000, A&A, 364, L62
More A., Suyu S. H., Oguri M., More S., Lee C.-H., 2017, ApJ, 835, L25
Oguri M., Kawano Y., 2003, MNRAS, 338, L25
Refsdal S., 1964, MNRAS, 128, 307
Riess A. G. et al., 2016, ApJ, 826, 56
Rubin K. H. R. et al., 2017, preprint (arXiv:1707.05873)
Rusu C. E. et al., 2017, MNRAS, 467, 4220
Sluse D., Hutsemékers D., Courbin F., Meylan G., Wambsganss J., 2012, A&A, 544, A62
Suyu S. H. et al., 2017, MNRAS, 468, 2590
Wisotzki L., Koehler T., Kayser R., Reimers D., 1993, A&A, 278, L15

This paper has been typeset from a TEX/LATEX file prepared by the author.